

Non-Hermitian approach of edge states and quantum transport in a magnetic field

B. Ostahie^{1,2}, M. Nița¹ and A. Aldea¹

¹ *National Institute of Materials Physics,
77125 Bucharest-Magurele, Romania.*

² *Department of Physics, University of Bucharest*

Abstract

We develop a manifest non-Hermitian approach of spectral and transport properties of two-dimensional mesoscopic systems in strong magnetic field. The finite system to which several terminals are attached constitutes an open system that can be described by an effective Hamiltonian. The life time of the quantum states expressed by the energy imaginary part depends specifically on the lead-system coupling and makes the difference among three regimes: resonant, integer quantum Hall effect and superradiant. The discussion is carried on in terms of edge state life time in different gaps, channel formation, role of hybridization, transmission coefficients quantization. A toy model helps in understanding non-Hermitian aspects in open systems.

PACS numbers: 73.23.-b, 05.60.Gg, 73.43.Cd

I. INTRODUCTION

Integer quantum Hall effect (IQHE) is a topological transport effect exhibited by the two-dimensional (2D) electron systems when subjected to a strong perpendicular magnetic field. The theoretical understanding of this effect followed two distinct routes. The first one starts with the Kubo formula for the conductivity of an infinite system, and adapts it for the case when the Fermi level sits in an energy gap between Landau levels [1]. The conductivity can be expressed as an integral over the Brillouin zone of the Berry curvature, and it turns out to be (in units e^2/h) a topological invariant known as the first Chern number specific to the given gap [2].

The second route, which is closer to the physical realization of the quantum Hall devices, puts forward the role of the *edge states* induced by the strong magnetic field in *confined* 2D electron systems. The equivalence of the two approaches is discussed in terms of bulk-edge correspondence.

The edge states exhibit chirality due to the broken time-reversal symmetry of the Hamiltonian and fill the gaps between the usual Landau bands. In this picture, as long as the Fermi level E_F sits in a gap, the current is carried by edge states. The transverse conductance exhibits plateaus $G_{xy}(E_F) = Ne^2/h$, where the integer N represents the number of edge states taking part in the transport. This conventional description of the IQHE is supported by the well-known energy spectrum of the 2D electron gas in the presence of hard wall edges (with strip or annular geometry), which is sketched in Fig.1 as function of the position of the guiding center X_0 [3–5]. The spectrum exhibits degenerate Landau-type levels in the middle of the strip, but shows dispersion close to the edges at $X_0 = \pm L/2$. The states located near the walls (i.e., the edge states) fill the gaps, the number of edge states at the Fermi level depending obviously on the gap index where E_F sits.

The description provided by the strip model is heuristic and far from experimental circumstances. It becomes more realistic by taking two more steps: i) to replace the infinite strip with a finite sample, described by a 2D plaquette with vanishing boundary conditions all around, and next ii) to open the system by attaching four semi-infinite leads necessary for injecting/collecting the electron current, and also for measuring the Hall voltage. If the leads are attached to the margin of the sample, the edge states *hybridize* with the electron modes in the semi-infinite leads and give rise to *scattering* states, which describe the elec-

tron propagation from one reservoir to other ones by passing through the sample [6, 7]. Before addressing the problem of open systems, we observe that the two above mentioned

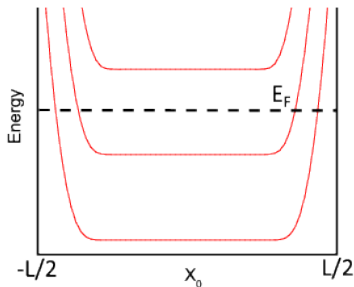


FIG. 1: Sketch of the energy spectrum of the 2D electron gas in perpendicular magnetic field with hard walls at $\pm L/2$.

routes are not prepared to take into account the role of the lead-sample coupling. Still, Fig.1 offers a hint, which usually is not remarked but is relevant in this respect: namely, the spatial distance of the edge states from the sample margin depends on their origin; more specifically, the states provided by the lower Landau bands are closer to the edges than those coming from the higher ones. This suggests that the hybridization of the lead modes with the edge states is not unique, but depends on the gap where the edge states are energetically located. In this context, we shall show how a poor hybridization affects the accuracy of the conductance quantization.

In the next section, we introduce the approach of the effective non-Hermitian Hamiltonian for the open systems and show how it works for an analytically solvable toy model. Sec.III explains three transport regimes of the 2DEG in strong perpendicular magnetic field in terms of the lead-sample hybridization and edge states lifetime, proving the presence of superradiant effects at strong coupling, beyond the quantum Hall regime. The conclusions can be found in the last section.

II. EFFECTIVE HAMILTONIAN AND ONE-DIMENSIONAL TOY MODEL

The Hamiltonian of the composed system can be written as the sum of terms describing the 2D finite sample (S), the leads (L) and the sample-leads coupling:

$$H = H^S + H^L + \tau_c(H^{SL} + H^{LS}), \quad (1)$$

where the coupling parameter τ_c is essential in the physics of open systems. From the point of view of the transport properties in strong magnetic field, the gradual increase of τ_c moves the system from the resonant regime, expressed by sharp peaks of the transmission coefficient, to the quantum Hall (QH) regime described by plateaus of the transmission (and, implicitly, of the Hall conductance). However, the study of some 1D open models indicates also the presence of a third regime in the limit of strong τ_c , where superradiance effects occur [8, 9]. Such kind of effects should be expected in the 2D open system described by (1) as well, and one may ask what new spectral and transport features may arise by increasing the coupling beyond the QH regime.

Superradiance phenomena in open systems are described in terms of non-Hermitian quantum mechanics, usually for one-dimensional models. The main topic of interest is the evolution with the coupling strength of the complex eigenvalues, and of the corresponding bi-orthogonal set of eigenfunctions. Effects as resonance overlapping, segregation of the eigenvalues or superradiance transition can be shown. Specific superradiance effects are also revealed by the quasiflat band in phosphorene [10].

The problem described by (1) can be cast into a non-Hermitian formalism by including the effect of the leads into an effective Hamiltonian for the finite sample. In this formalism, the evolution of the eigenvalues in the complex plane as function of τ_c , combined with the degree of hybridization of the edge states with the lead modes, provides a unified description of the three transport regimes: resonant, quantum Hall and superradiant. The approach allows to visualize the track of electrons in the sample for all these regimes, and to get an understanding of the QHE beyond the heuristic picture.

Technically speaking, the non-Hermitian effective Hamiltonian H_{eff}^S that describes the finite sample in contact with leads can be obtained by the formal elimination of the leads degrees of freedom using a projection procedure. When projected on the lead and plaquette subspaces, the Hamiltonian (1) reads as the following 2×2 matrix:

$$\mathbf{H} = \begin{pmatrix} H^S & \tau_c H^{SL} \\ \tau_c H^{LS} & H^L \end{pmatrix}. \quad (2)$$

A way to prove the structure of H_{eff}^S describing the plaquette in contact with the leads is via the Green function defined as $\mathbf{G}(z)(z\mathbf{1} - \mathbf{H}) = \mathbf{1}$. By projecting this equation on the

two subspaces, the following system of equations is obtained:

$$\begin{aligned} G^{SS}(z-H)_{SS} + G^{SL}(z-H)_{LS} &= 1, \\ G^{SS}(z-H)_{SL} + G^{SL}(z-H)_{LL} &= 0. \end{aligned} \quad (3)$$

It results immediately $G^{SS}(z)(z-H_{eff}^S) = 1$ with

$$H_{eff}^S(z) = H^S + \tau_c^2 H^{SL}(z-H^L)^{-1} H^{LS}, \quad (4)$$

where one notes that the effective Hamiltonian is non-Hermitian and dependent on the complex energy z .

In order to continue, the explicit expressions of H^S, H^L and H^{LS} are necessary. In the tight-binding description, introducing the creation (annihilation) operators $c_n^\dagger (c_n)$ on the sites $\{n\}$ of the lattice, one may write:

$$H^S = \sum_{n,n'} t_{n,n'} e^{i\phi_{n,n'}} c_n^\dagger c_{n'}, \quad (5)$$

where $t_{n,n'}$ is the hopping integral, and $\phi_{n,n'}$ stands for the Peierls phase in the presence of the perpendicular magnetic field. The energy spectrum of the confined (non-interacting, spinless) electronic system described by (5) is a Hofstadter-type butterfly, where the energy gaps are filled with edge states.

While the processes of interest occur in the plaquette, the role of the leads is to inject (and collect) independent electrons in the 2D plaquette. Along with Büttiker [11], each lead contains several independent channels, which are modeled by semi-infinite one-dimensional chains:

$$H^L = \sum_{\alpha=1}^4 H_\alpha^L, \quad H_\alpha^L = t_L \sum_{\nu=1}^{N_c} \sum_{i \geq 1} a_{\alpha,\nu,i}^\dagger a_{\alpha,\nu,i+1} + H.c., \quad (6)$$

where α counts the leads, ν counts the channels in the given lead, and i stands for the site index in the tight-binding description of the chains. Next, the lead-sample coupling Hamiltonian can be written as:

$$H^{LS} = \sum_{\alpha,\nu} c_{\alpha,\nu}^\dagger a_{\alpha,\nu,1}, \quad H^{SL} = H^{LS\dagger}. \quad (7)$$

This expression says that the first site $i = 1$ of the channel ν in the lead α is stucked to the sample site denoted by (α, ν) . The summation over all channels and leads is performed.

The parameter τ_c represents the coupling strength and is essential for the transport in meso-systems and superradiance physics in open systems.

Combining Eqs.(5-7) with Eq.(4), after some straightforward algebra, the following explicit formula of the effective Hamiltonian is obtained:

$$H_{eff}^S = H^S + \frac{\tau_c^2}{t_L} e^{ik} \sum_{\alpha,\nu} c_{\alpha,\nu}^\dagger c_{\alpha,\nu} . \quad (8)$$

The above Hamiltonian, being non-Hermitian, exhibits complex eigenvalues. In addition, it depends on the energy E of the incoming electrons via the quantity k in (8) that parametrizes the energy as $E = 2t_L \cos k$. At this stage, before addressing the problem of the 2D plaquette

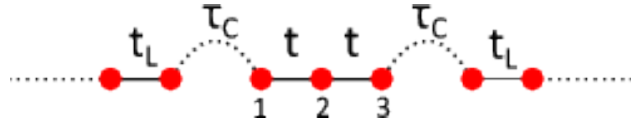


FIG. 2: Schematic description of a toy model with three sites. The first and last site are connected to semi-infinite leads.

with several multi-channel leads, the discussion of a simple analytically solvable model is useful for understanding the influence of the lead-sample coupling on the complex spectrum and electron transmission coefficient. Let us consider the short chain composed of three sites, two of them being connected to semi-infinite leads via the parameter τ_c , as in Fig.2. For this system, the effective Hamiltonian reads in the matrix form as:

$$H_{eff}^S = \begin{pmatrix} \frac{\tau_c^2}{t_L} e^{ik} & t & 0 \\ t & 0 & t \\ 0 & t & \frac{\tau_c^2}{t_L} e^{ik} \end{pmatrix} . \quad (9)$$

We have to remark that the non-Hermitian models mostly studied in the literature exhibit PT-symmetry [12, 13], in which case there are values of τ_c for which the spectrum is real. On the contrary, the effective Hamiltonian (9) shows broken PT-symmetry, and its spectrum is always complex, the eigenvalues being:

$$\omega_0 = i\tau_c^2/t_L, \quad \omega_{\pm} = \frac{1}{2}(\omega_0 \pm \sqrt{8t^2 - (\tau_c^2/t_L)^2}) , \quad (10)$$

where, for simplicity, we have chosen $k = \pi/2$.

The real and imaginary part of the three eigenvalues are shown in Fig.3 as function of τ_c . One notices the coalescence of the three branches of $\text{Re } \omega$, and also the bifurcation of $\text{Im } \omega$

at $\tau_c^2 = 2\sqrt{2}tt_L$, which is known as an *exceptional point* (EP) in the spectrum. (We noticed the EP occurs only for odd numbers of sites in the chain, but such aspects are beyond the main topic of the paper.)

It is important to underline that the imaginary part of two eigenvalues increases unboundedly with increasing τ_c , generating what is called *superradiant* states. At the same time, the third one decreases to zero. In other words, the width $\Gamma = \text{Im}E$ of two resonances increases indefinitely, while the third one becomes thinner and thinner with increasing coupling. Such spectral properties are specific to superradiance, and our aim now is to find out how they are reflected in the transport properties. By calculating the Green function

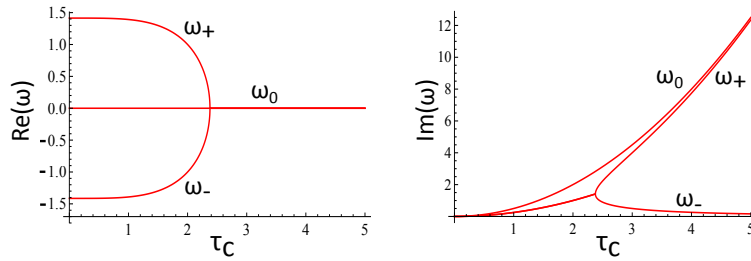


FIG. 3: The real and imaginary part of the eigenvalues (10) as function of the coupling parameter τ_c ($t = 1$, $t_L = 2t$).

that corresponds to the Hamiltonian (9), the transmission coefficient is obtained immediately from $T = 4(\tau_c^4/\tau_L^2)|G_{13}^{SS}|^2 \sin^2 k$, which is the particularization of (11) for the case of only two contacts. The result is depicted in Fig.4 as function of the gate potential and coupling parameter. (The Fermi level is fixed in the leads at $E_F = 0$, and it is tuned to different spectrum domains by a gate potential applied on the sample, which can be varied continuously. The gate is simulated in the Hamiltonian by a diagonal term $V_g \sum_n c_n^\dagger c_n$.) One has to observe in Fig.4 the presence of three resonant peaks at small τ_c and of a single narrow peak that corresponds to the state ω_- at large τ_c , showing that the highly broadened superradiant states do not contribute to the transmission. Another highly interesting thing is the formation of the plateau $T = 1$ at a value of the coupling which is below, but close to the exceptional point. Thus, we learn from this toy model that the increase of the lead-sample coupling yields the broadening of the peaks, such that their overlapping give rise to a transmission plateau. Then, by increasing the coupling further on, the plateau is spoiled, and the system reenters a specific resonant regime, described by a single peak, where the superradiant states are no more visible in the transmission.

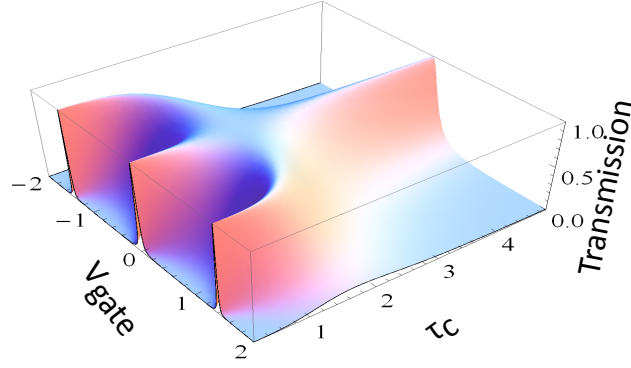


FIG. 4: The transmission coefficient T of the toy model as a function of the gate potential and coupling strength.

In what follows, we approach the problem of the 2D electron system in magnetic field, looking for similar effects and their implications for the quantum Hall effect.

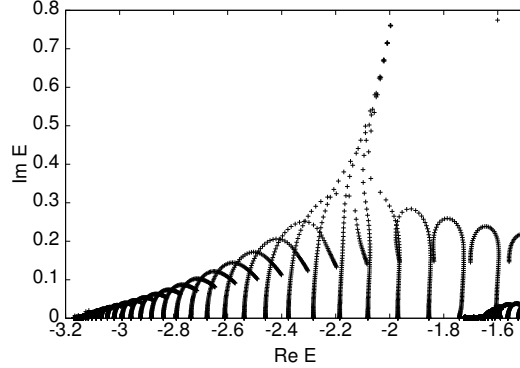


FIG. 5: The evolution with increasing τ_c of the eigenvalues in the complex plane, corresponding to edge states in the first gap. The turning point of the *hooks* occurs at $\tau_c \approx 1.5t$. The superradiant states are also visible. (The plaquette dimension is 21×21 sites, and the magnetic flux through the unit cell is $\Phi = 0.15\Phi_0$, Φ_0 = magnetic flux unit.)

III. TWO-DIMENSIONAL OPEN SYSTEM IN STRONG MAGNETIC FIELD

The first relevant effect is the dependence on the coupling τ_c of the complex eigenvalues of H_{eff}^S shown in Fig.5. It is to observe that, the leads being attached at the boarder of the plaquette, only the edge states eigenvalues are significantly affected. Both the real and

imaginary part are shifted with increasing τ_c , two aspects being remarkable: i) the expected initial increase of ImE is followed at stronger coupling by a decrease that gives rise to a hook shape, and ii) the emergence of superradiant states, whose imaginary part increases unboundedly with increasing coupling. Both these characteristics are met also in 1D models and considered as typical for non-Hermitian Hamiltonians [9].

The Hall conductance of a *four-lead* device can be derived using the Landauer-Büttiker formalism, which involves the numerical calculation of all transmission coefficients between different leads $T_{\alpha,\alpha'}$ ($\alpha, \alpha' = 1, \dots, 4$). The formalism asserts that the formation of the IQHE plateaus is conditioned by integer values of the transmission coefficients $T_{\alpha+1,\alpha}$ between consecutive leads, and zero values for all the others. It is obvious that for pinched contacts (i.e., in the limit $\tau_c \rightarrow 0$) the system works in the resonant regime. The question then arises how strong the coupling should be in order for the QH regime to occur. In terms of the Green function, $T_{\alpha,\alpha'}$ is given by the known Caroli expression [14]:

$$T_{\alpha\alpha'} = \frac{4\tau_c^4}{t_L^2} \sum_{\nu,\nu'} |G_{\alpha\nu,\alpha'\nu'}^{SS}|^2 \sin^2 k, \quad \alpha \neq \alpha'. \quad (11)$$

(Let us remind that *sink* in (11) comes from the density of states in the leads.) The result

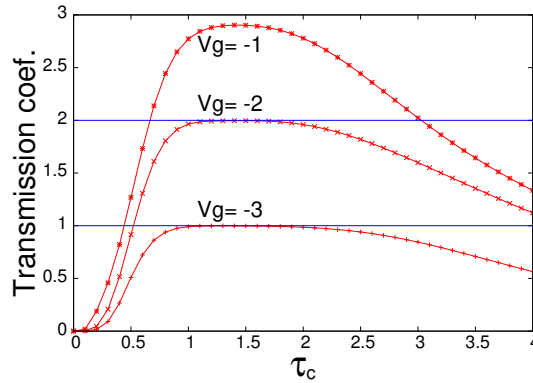


FIG. 6: T_{21} as function of τ_c for different values of the gate potential which fits the Fermi level in the first three gaps. (The plaquette dimension is 40×20 sites, $\Phi = 0.1\Phi_0$.)

of the numerical calculation of T_{21} as function of τ_c is shown in Fig.6 for three different positions of E_F in the first three gaps. One should notice that the range of τ_c that ensures the transmission quantization shrinks when moving to higher gaps, and already in the third one the expected value $T_{21} = 3$ is no more perfectly reached. This effect is symptomatic, and it can be understood in terms of imperfect channels due to insufficient hybridization

of the lead modes to the innermost edge state. The smaller the plaquette is, the easier this outcome can be evidenced. One has also to observe the decrease of the transmission at high coupling, announcing the decay of the IQHE and the reentrance of a resonant-type regime. Aiming to understand the result in Fig.6, we discuss the life time defined by the inverse of the energy imaginary part $\tau = \hbar/ImE$, and also the path followed by the electron inside the sample for the different transport regimes we come across.

Let us assume that the electron enters the sample along a given lead α . The coupling term $H^{SL} + H^{LS}$ hybridizes the lead eigenfunction $|\Phi_\alpha^L\rangle$ with those of the sample and generates the scattering wave function $|\Psi_\alpha\rangle$ described by the Lipmann-Schwinger expression: $|\Psi_\alpha\rangle = |\Phi_\alpha^L\rangle + GV|\Phi_\alpha^L\rangle$, with $V = H - H_\alpha^L$. Then, the electron path through the sample can be visualized by the projection of $|\Psi_\alpha\rangle$ on *all* sample sites $|\langle n|\Psi_\alpha\rangle|^2$. As technical aspects, we mention that from all terms in V only H^{SL} contributes, while the Green function G , being projected on the sample sites, should be replaced by G^{SS} . One obtains readily:

$$|\langle n|\Psi_\alpha\rangle|^2 = \tau_c^2 \sum_\nu |\langle n|\frac{1}{V_g - H_{eff}^S}|\alpha, \nu\rangle|^2, \quad n \in S, \quad (12)$$

where $|\alpha, \nu\rangle = c_{\alpha, \nu}^\dagger|0\rangle$, and again V_g is the gate potential.

Let us discuss first the resonant regime. In this case, the edge states of the isolated sample (described by H^S) are weakly perturbed by the leads, so that the imaginary part acquired by the complex eigenvalues of H_{eff}^S is small (more precisely, $ImE \ll \Delta$, where Δ is the mean level spacing between consecutive edge states). Correspondingly, the life time of the injected electron in the sample is long, meaning that the electron can get out of the sample with significant probability at any contact. The consequence is that, in the resonant regime, all $T_{\alpha, \alpha'}$ are different from zero. Further support to this picture comes from the charge distribution on the plaquette given by Eq.(12), which turns out to be distributed all around the perimeter (as shown in Fig.7a), similarly to the edge state in the isolated plaquette. (The life time is the time spent by electron in the sample, so that equivalently one may use also the term 'escape time' as in [15].)

The increase of τ_c results in reducing the life time and shortening the electron path in the sample as shown in Fig.7b. Expecting to reach the QH regime, we increase the coupling further on, and, indeed, one arrives at the situation when the scattering wave that enters the contact α leaves the sample at the next contact $\alpha + 1$, as obvious in Fig.7c. Then, $T_{\alpha+1, \alpha}$ is the only non-vanishing transmission coefficient and equals an integer. This is just the

requirement for the realization of the quantum plateau.

The construction of the scattering wave function is different for the two cases discussed above. If $ImE \ll \Delta$, the density of energy states in the sample shows a peak structure, and the scattering wave function results from the hybridization of the lead mode with the edge state that satisfies the resonance condition. On the other hand, if $ImE \sim \Delta$, due to the level broadening, the scattering wave function is built by weighted contribution of different edge states. In this case (which occurs by increasing the coupling τ_c), the density of states becomes a smooth function of energy in the whole energy range covered by edge states, and the same occurs for the transmission coefficient, meaning that we have reached the QH regime. As we already mentioned, the toy model reveals a similar behavior of the transmission in Fig.4.

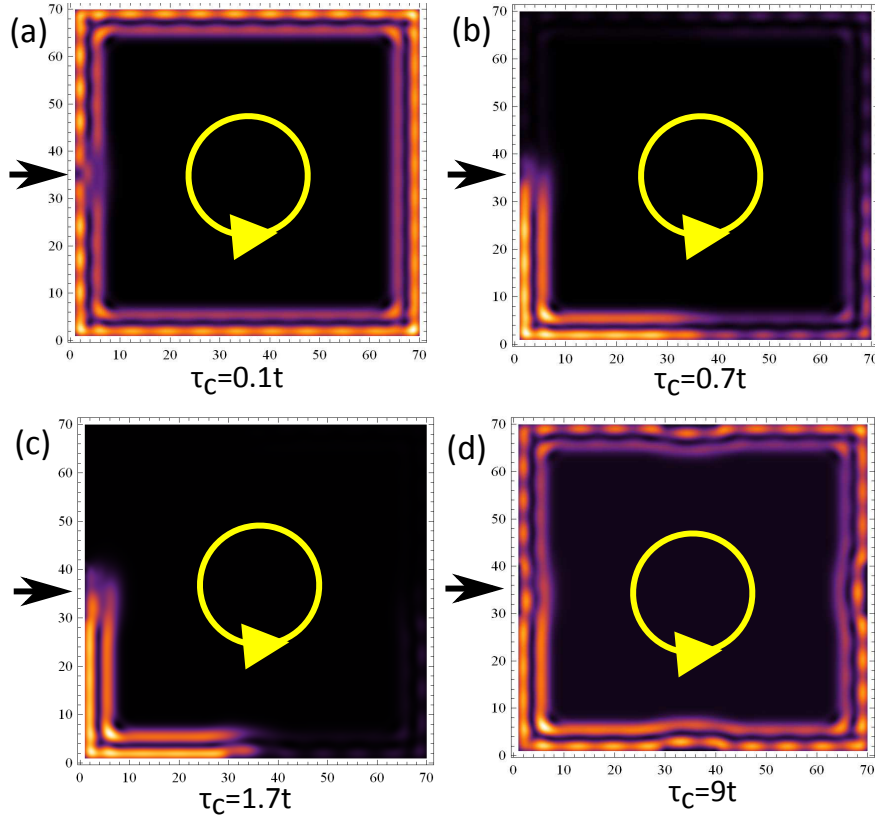


FIG. 7: The path (in red) followed by electrons in a square plaquette with four leads for different couplings τ_c , which correspond to different regimes. The injection place is indicated by black, and the path chirality by yellow arrows. E_F is tuned in the second gap. (The plaquette dimension is 70×70 sites, each lead contains 10 channels, and $\Phi = 0.04\Phi_0$.)

The limit of the very strong coupling, known in the physics of open systems as the superradiant regime, was not yet studied from the point of view of the quantum transport properties in 2D systems. We know already from Fig.5 and Fig.6 that, for high values of τ_c , the life time increases again, while the transmission coefficient decreases below the integer values. In addition, one may observe in Fig.7d that the electron path is enlarged again and keeps the plaquette perimeter similarly to the resonant regime. These circumstances suppress the IQHE plateaus, and the numerical calculation indicates that they are replaced by transmission oscillations when V_g is varied.

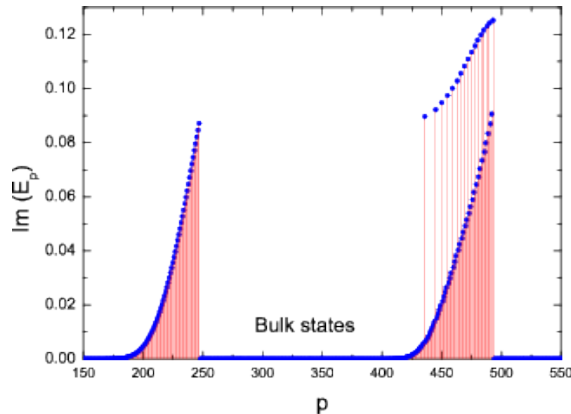


FIG. 8: The imaginary part ImE_p as function of the eigenvalue index p in the spectral range of the first two gaps. The parameters are the same as in Fig.7, $\tau_c = 1.7t$.

We are still left with the question concerning the formation of many channels in the higher gaps; without loss of generality, we restrict the discussion to the second one. Fig.8 strings the widths of all edge states in the first two gaps. The apparently empty range $p \in [250, 420]$ is in fact occupied by bulk band states which, as mentioned already, show vanishing width. The important issue is that the values of ImE_p in the second gap segregate into two sets, proving the existence of two types of edge states distinguished by their width. The calculation being performed at given τ_c , we conjecture that the segregation originates in the different hybridization of different types of edge states existing in the gap. Obviously, the higher widths comes from a stronger hybridization and should correspond to edge states localized closer to the margin. According to the hint given by the heuristic model Fig.1, they can be associated to the edge states detached from the first Landau band. Similar reasoning says that the family of states with low width are more remote from the margin and correspond to the states provided by the second band.

One may further speculate that in the higher gaps there are edge states localized far away from the margin, having a small overlap with the lead modes and a long life time. Then, the corresponding channels do not get out of the sample at the next contact and spoils the quantized value of the transmission, giving rise to imperfect QHE plateaus of higher index. This is the case in Fig.6 for the third gap. The appearance of such deviations from the very well quantized plateaus depends on different parameters like the plaquette dimension, value of τ_c or magnetic field strength.

IV. CONCLUSIONS

In summary, we highlighted the determinant role of the edge states lifetime in defining different transport regimes in open systems: resonant, quantum Hall and superradiant. The lifetime is defined by the imaginary part of the complex eigenvalues of the non-Hermitian effective Hamiltonian that describes the 2D finite sample in contact with leads. The lead-sample coupling induces a specific evolution of the eigenvalues in the complex plane and controls the conditions for emergence of the IQHE and superradiant regime (which appears *beyond* the QH regime, in the limit of high coupling). We used the model Hamiltonian (1), however we think that the qualitative physical results are generally valid.

Although deduced for finite 2D electron gas in magnetic field, our considerations are applicable to all materials exhibiting edge/surface states, including those recently discovered in the topological insulators.

A difficult question is under what circumstances the superradiant regime can be seen experimentally. In principle, the solution is to decrease the hopping parameter t , that is to use narrow band materials. However, at that moment the correlations become important, and the one-particle description used here becomes questionable. Of course, the superradiant effects combined with the fractional Hall effect would be highly interesting, however it is much beyond our present aim. Then, an alternative would be to decrease t_L , meaning leads with heavy electron effective mass.

V. ACKNOWLEDGMENTS

We acknowledge the financial support from Romanian Core Research Programme PN16-480101.

- [1] P Streda, J. Phys. C : Solid State Phys. **15** L1299 (1982).
- [2] D. J. Thouless, M. Kohmoto, M. P. Nightingale, and M. den Nijs, Phys. Rev. Lett. **49**, 405 (1982).
- [3] B. I. Halperin, Phys. Rev. B **25**, 2185 (1982).
- [4] R. E. Prange, in *The Quantum Hall Effect* edited by R. E. Prange and S. M. Girvin, Springer Verlag , 1987.
- [5] A. H. MacDonald and P. Streda, Phys. Rev. B **29**, 1616 (1984).
- [6] H. U. Baranger and A. Douglas Stone, Phys. Rev. B **40**, 8169 (1989).
- [7] M. Janssen, Solid State Comm. **79**, 1073 (1991).
- [8] G. L. Celardo and L. Kaplan, Phys. Rev. B **79**, 155108 (2009).
- [9] Y.S. Greenberg, C. Merrigan, A. Tayebi, and V. Zelevinsky, Eur. Phys. J. B **86**, 368 (2013).
- [10] B. Ostahie and A. Aldea, Phys. Rev. B **93**, 075408 (2016).
- [11] M. Büttiker, Y. Imry, R. Landauer, and S. Pinhas, Phys. Rev. B **31**, 6207 (1985).
- [12] C. M. Bender, Rep. Prog. Phys. **70**, 947 (2007).
- [13] I. Rotter, J. Phys. A: Math. Theor., **42**, 153001 (2009).
- [14] C. Caroli, R. Combescot, P. Nozieres, and D. Saint-James, J. Phys. C: Solid St. Phys. **4**, 916 (1971).
- [15] S. Datta, *Electronic Transport in Mesoscopic Systems*, ch.3, Cambridge University Press, 1995.